International Journal of Disaster Risk Reduction 111 (2024) 104734

Contents lists available at ScienceDirect

International Journal of Disaster Risk Reduction

journal homepage: www.elsevier.com/locate/ijdrr

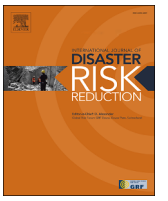

Innovative steel modular housing system for multiple natural hazard mitigation

Luigi Di Sarno [a, *], Roberto Forgione [b]

[a] Department of Civil and Environmental Engineering, University of Liverpool, Liverpool, UK
[b] Department of Civil and Environmental Engineering, University of Illinois at Urbana-Champaign, Urbana, IL, USA

ARTICLE INFO

Keywords:
Flood risk management
Modular systems
Property level flood-risk mitigation measures
Resilience
Risk mitigation

ABSTRACT

Floods are among the most destructive natural disasters threatening lives, communities, and economies, with annual damage reaching billions of pounds worldwide. Human activities and recent climate emergencies are exacerbating the frequency and severity of these catastrophic events, exposing large communities to the risk of such natural hazards. Various mitigation techniques at both community and property levels can be adopted to provide responsive solutions for natural threats. In this study, a transformative steel modular housing system capable of rising above the ground in the event of a flood is presented. The robustness and efficiency of such an innovative system were tested on a full-scale prototype at the state-of-the-art HR Wallingford testing facility for flood resilience in the UK. To extend the applicability and assess the reliability of the innovative flood-resilient system, a comprehensive numerical investigation was carried out to check whether the modular system can reliably withstand multiple natural hazards, such as flooding, strong winds, and seismic ground motions. A refined numerical model was first calibrated on the basis of experimental outcomes to create a digital twin of the tested building. Such a model was then used to demonstrate the effectiveness of the proposed modular steel building under different flooding scenarios, i.e., in configurations with increasing height above the ground, namely 300 mm, 600 mm, and 900 mm. The results of experimental tests and the comprehensive parametric numerical analyses demonstrate that the proposed newly developed steel modular housing system ensures structural integrity, adequate performance, and resilience even for extreme flood scenarios characterised by rapid water velocities and severe wind conditions. The innovative and resilient modular housing system presented has also been demonstrated to be reliable for areas with moderate seismicity, i.e., with peak ground accelerations lower than 0.25 g. The proposed resilient and sustainable adaptation technology can thus be employed efficiently in regions worldwide that are exposed to multiple natural hazards, e.g., floods, high winds, and earthquakes.

1. Introduction

Floods are among the most severe natural disasters, annually resulting in thousands of deaths, millions of people affected, and billions of pounds in total damages worldwide. From 1960 to 2023, there have been more than 200 flood events globally, causing a minimum of 100 fatalities and impacting approximately 500,000 individuals collectively. In addition, floods have caused damage exceeding £1 million adjusted for inflation on more than 270 occasions (Fig. 1) [1]. In 2022, floods ranked second among the most impactful

* Corresponding author.
E-mail addresses: luigi.di-sarno@liverpool.ac.uk (L. Di Sarno), rocaf397@illinois.edu (R. Forgione).

https://doi.org/10.1016/j.ijdrr.2024.104734
Received 17 December 2023; Received in revised form 30 July 2024; Accepted 5 August 2024
Available online 6 August 2024
2212-4209/© 2024 Elsevier Ltd. All rights are reserved, including those for text and data mining, AI training, and similar technologies.

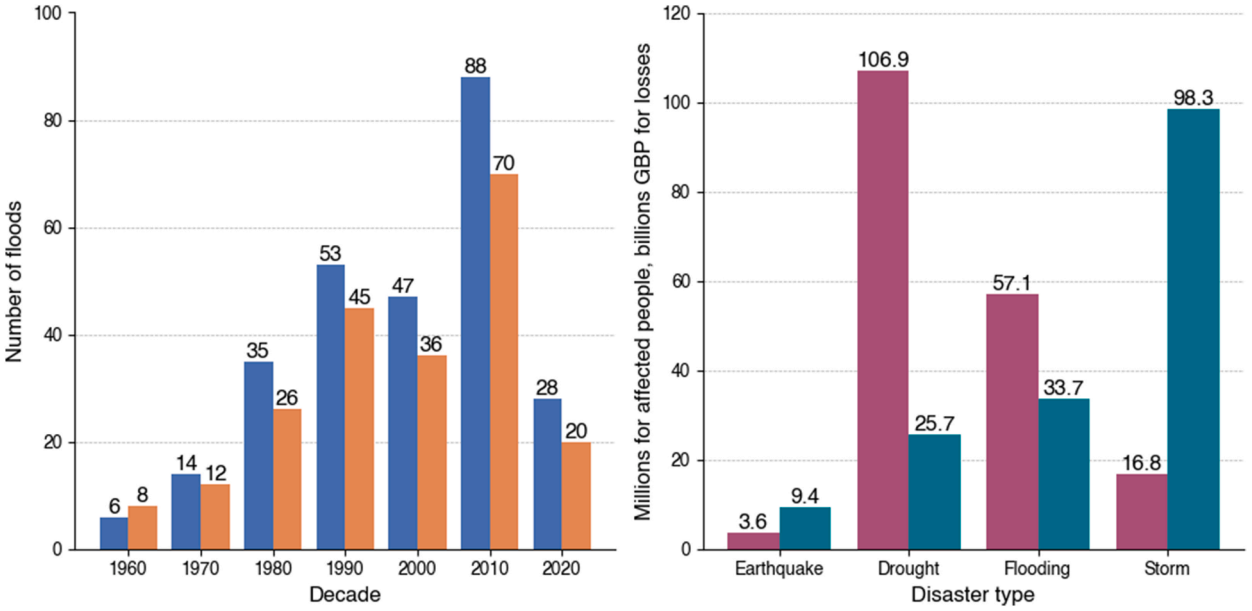

Fig. 1. Statistics on the effects of flooding: left) Number of floods that caused at least 100 deaths and impacted more than 500,000 people (blue) and number of floods that caused more than £1,000,000 adjusted for inflation in damage (orange); right) Number of affected people (purple) and economic losses (teal) for earthquakes, droughts, floods, and storms in 2022. Note: The statistics for the 2020 decade are as of June 2023. (For interpretation of the references to colour in this figure legend, the reader is referred to the Web version of this article.)

natural disasters worldwide, both in terms of the number of people affected and the economic damage incurred, placing just behind droughts and storms respectively (Fig. 1) [2]. Relevant flood events occurred recently in Italy from 17 to 23 May, 2023 (17 deaths, 50,000 affected, £5.5 billion damage) (Fig. 2a), Haiti from 2 to 3 June, 2023 (51 deaths, 30,000 affected), which at the same time coped with two earthquakes of magnitude between 5 and 6 M_W, Pakistan (2035 deaths, £3.9 billion damage) (Fig. 2b), and Eastern Australia (£5.2 billion damage).

Although previous data emphasise flooding hazards globally, it is worth noting that many floods, particularly in developing countries, might not be reported or are underreported, resulting in an underestimation of the real impact of floods on a global scale [3]. Insurance companies usually cover just a small portion of the damage caused by floods. Less than a quarter of the £42 billion losses registered across Europe due to flooding in 2021 were insured [4] and just a minor part of the £12 billion losses caused by the last-year Pakistani flash floods were covered [5].

The increasing flood risk poses pressing threats to social communities globally, as many cities are compelled to expand and construct buildings in flood-prone areas. Numerous residential buildings are also exposed to flood threats. One in six homes in the UK is at risk of flooding, and in England alone half a million properties are located in areas of annual probability of flooding higher than 1% [6]. The problem is exacerbated by man-made activities such as urbanisation and development in flood-prone regions [7,8], excessive land use leading to water retention, and the impact of climate change [9–11].

Weather forecasts indicate that climate change will significantly amplify the frequency and intensity of floods. By the end of this century, flood events that were previously considered to occur once in a hundred years in the 20th century will happen every 10–50 years [12]. This escalating frequency of floods poses an additional serious threat to densely populated areas worldwide [13], which may become unsafe or uninhabitable and necessitate the relocation of affected communities [14].

Numerous strategies for mitigating and adapting to flood risk have been proposed globally [15–19]. These strategies can be categorised based on whether they aim to protect entire communities or individual properties. Community-level mitigation techniques (CLMTs) are designed to protect whole communities and are typically situated near bodies of water, making them more cost-effective

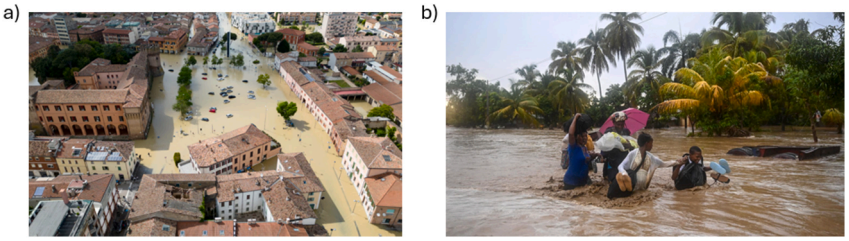

Fig. 2. Recent floods occurred worldwide: a) Floods occurred in the northeast of Italy from 17 to 23 May, 2023; b) Haiti from 2 to 3 June, 2023.

for densely populated areas [20]. Conversely, property-level mitigation techniques (PLMTs) involve modifications to individual properties and are generally more suitable for less densely populated areas.

CLMTs include dams, levees, and sluice gates designed to prevent water overflow during extreme rainfall. Channelisation helps manage rainwater flow, diverting it away from populated areas. Other CLMTs involve river treatment, including maintenance, retention, floodplain restoration, and floodwater diversion and storage. These techniques have proven to be effective in significantly reducing flood-prone areas [21,22]. However, CLMTs alone are insufficient, as significant losses still occur during floods without PLMTs [23,24]. Therefore, combining PLMTs with CLMTs is optimal for comprehensive flood risk management [13,25].

PLMTs vary in cost and feasibility depending on whether they are applied to new or existing buildings and across different geographic regions. Their effectiveness also depends on the characteristics of the floods, such as high-velocity flooding dominated by hydrodynamic and debris actions, or groundwater flooding where hydrostatic and buoyancy actions are more significant [26]. PLMTs can be categorised into three groups, as shown in Fig. 3: flood avoidance, flood resistance, and flood resilience.

Flood avoidance consists of measures designed to prevent floodwaters from reaching properties or to minimise the impact of flooding when it occurs. PLMTs such as landscape design, building elevation, and constructing on elevated ground are highly effective and reliable in reducing flood risks. Landscape design, including site drainage and surface water runoff management, adapts the surrounding area to lower flood risk and is cost-effective for the community [27,28]. Building on elevated ground during the development of new constructions is another reliable method, ensuring that properties are less prone to flooding [29]. Raising existing buildings above flood levels is a permanent solution that significantly mitigates flood risk [30]. While elevation is more cost-effective during the construction phase, it remains a viable option for retrofitting existing structures, though it can be more expensive for masonry buildings compared to wooden ones [31,32]. Collectively, these measures provide robust flood protection, but it is crucial to consider their impact on adjacent properties to avoid transferring flood risk [33].

Flood resistance encompasses mitigation techniques designed to protect structures by either allowing controlled water entry and exit (wet flood-proofing) or preventing water from entering entirely (dry flood-proofing), thereby minimising structural damage during flooding events. Wet flood-proofing, which allows floodwaters to enter a building, is generally less costly and requires less construction space. It can significantly reduce damage, with studies showing damage reductions of up to 53% for flood-adapted interiors [32]. However, it necessitates periodic maintenance and clean-up, and its effectiveness diminishes for flood depths exceeding 2 m [34]. Conversely, dry flood-proofing aims to prevent water entry altogether, making it more effective for lower water depths (up to 1 m) and capable of reducing damage by up to 60% [32]. While dry flood-proofing is more costly—estimated to be 2.5 times more expensive than wet flood-proofing [35] —it provides robust protection, especially when regularly maintained. Examples of effective dry flood-proofing measures include sealed light shafts, flood-proof basement windows, and waterproof cellars using bitumen or concrete seals. Both wet and dry flood-proofing require careful planning to ensure long-term effectiveness and to avoid increasing flood risks to adjacent properties.

Flood resilience encompasses techniques designed to minimise the impact on a structure when floods occur, ensuring the building remains undamaged. Examples are floating and amphibious houses, which are not fixed to the ground and can move vertically as the water level rises during a flood. Such techniques, which rise with floodwaters, offer an innovative and resilient alternative, especially in areas prone to seasonal flooding, though they are less common and more costly in some regions [28,36]. Additionally, temporary vertical lifting techniques involve houses changing height depending on flooding conditions, achieved through mechanical systems that enable them to rise. The innovative Flood Adaptive Platform (FAP) system for modular steel buildings presented herein falls within this category.

All the mitigation techniques discussed so far are structural, aiming to actively protect communities or individual properties. They can be complemented by non-structural mitigation techniques, such as early warning and forecasting systems that alert users to imminent floods, allowing evacuation before the event. Additionally, awareness programmes educate people on coping with floods. However, these non-structural techniques alone are insufficient to address flood risk.

2. Flood Adaptive Platform sustainable and resilient modular system

The innovative FAP system is designed to increase resilience by elevating the structure during flood events, as it ensures that the superstructure does not come into direct contact with the floodwater (flood-resilience as displayed in Fig. 3). This flood mitigation and adaptation strategy employs a mechanical system utilizing high-strength steel jacks to raise the structure during flooding, thereby preventing any contact between the building's superstructure and the flowing water. What sets the newly developed FAP system apart

Fig. 3. Flood mitigation and adaptation strategies for residential buildings.

from conventional house lifting methods discussed in the previous section is its automation. This is achieved using piezometers installed on the external perimeter of the steel modular system (see Fig. 8), which detect the presence and rising levels of water during flooding. Additionally, the uplifting system can be remotely controlled, allowing the superstructure to be elevated from a distance when necessary. This safe and reliable FAP system ensures that the structure can remain aesthetically intact with no damage, while also allowing occupants to stay safely and comfortably in the building during a flood event, as showed in Fig. 4.

2.1. Geometry of the proposed Flood Adaptive Platform modular system

The proposed modular system consists of three main components: a superstructure (building for residential occupancy), a steel grillage basement, and a mechanical jacking system (Fig. 5). The sample typical superstructure used for modular residential occupancy is designed according to Eurocode 3 [37]. It consists of a two-storey building structure with a plan layout of approximately 5.90 m by 9.60 m; the storey height is 2.60 m and the total building height is 8.80 m. The lightweight roof is a typical pitched roof with slopes of approximately 35°; it is made of plywood and covered with roof tiles.

The superstructure includes horizontal slabs made of cold-formed steel (CFS) that act as rigid diaphragms hence they limit the horizontal relative lateral displacements. Gypsum plasterboards are used for interior partitions and stairs with a thickness of 22 mm. The superstructure skeleton consists of 2 mm and 3 mm thick U-shaped CFS components, joined together through bolts and welds. The exterior cladding (façade) is constructed from masonry tiles. These tiles are designed to hold sensors that can serve as early warning systems. Additionally, such sensors have the capability to self-harvest energy from the vibrations of the cladding panels. Aluminium-framed doors and windows are installed on both floors and short sides of the house (Fig. 6).

The superstructure of the FAP system exhibits a rectangular shape with a ground floor layout comprising a typical residential architectural layout with a dining room, kitchen, toilet and living room (Fig. 7a). From the living room, a hallway leads to the staircase

Fig. 4. Remote Flood Adaptive Platform system lifting.

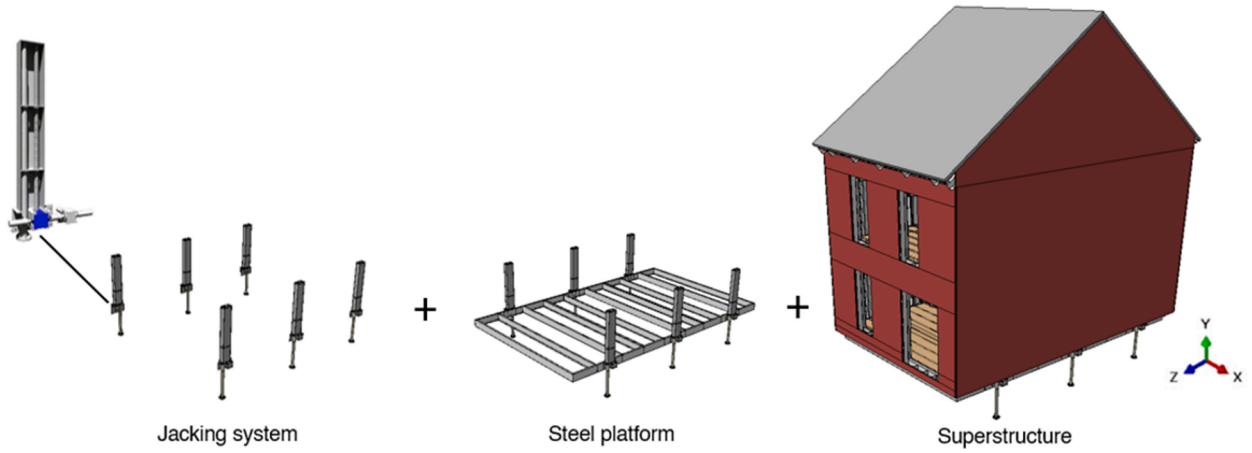

Fig. 5. Main components of the FAP system for residential modular buildings.

Fig. 6. FAP system tested in full scale at the state-of-art testing facility (HR Wallingford in Oxfordshire, UK).

accessing the second floor. On the second floor, there are three bedrooms, one of which features an ensuite bathroom, while the others share a separate bathroom (Fig. 7b). This building system is widely adopted in off-site modular construction in the United Kingdom and can be based on Design for Manufacturing and Assembly (DFMA) principles. Such type of prefabricated building system is indeed highly efficient due to its low-carbon, sustainable, and resilient building solutions for residential development [38,39].

The superstructure is connected to the metal base grid using bolts, through dry steel connections. The steel base grillage comprises U-shaped elements with 2 mm and 3 mm thicknesses; such elements have adequate stiffness to ensure functionality and stability for the superstructure. Six steel screw jacks are arranged in two rows along the superstructure's long side and connected to it through bolts on metal plates. The jacks have a hollow, circular cross-section with an external diameter of 101 mm, a thickness of 19 mm, an internal diameter of 82 mm, and a height of approximately 1900 mm.

Due to the geometric and mechanical properties of high-strength steel grade S600 (yield strength $f_y = 600$ MPa) used as a structural material, each jack has an axial capacity of about 2900 kN. The jacks employ hollow cross-sections and allocate an inner steel threated bar (Fig. 6). Such bar is a movable cylindrical element connected with its head through a steel, threaded vertical element which has a diameter of 55 mm. The jack, its movable part and the threaded vertical element are contained within the screw jack cover. The steel mechanical jacks are restrained at their base to prevent any movements (both displacements and rotations are prevented to achieve full fixity) and are operated by a centrally arranged motor connected to horizontal tubular elements on each side, allowing their simultaneous lifting.

Depending on soil-bearing capacities, the foundation system can consist of either deep foundations (e.g., steel or reinforced concrete piles) or shallow foundations (concrete mat or grid of reinforced concrete strip beams). The jacks are connected rigidly to the foundation system.

All architectural finishes and services (mechanical, electrical, etc.) used for FAP modular buildings can be easily accommodated by relying on similar technologies adopted in earthquake engineering solutions, e.g., in buildings with seismic base isolation systems. The total weight of the FAP system is about 30 tons.

In accordance with Eurocode 3 [37], beam and column cross-sections are classified as Class 4, thus indicating reduced resistance to bending and axial loads. The steel jacks, conversely, are Class 1 sections, thus they can reach full plastic capacity without local buckling occurrence. The geometric characteristics of the structural elements are presented in Table 1, while the mechanical characteristics of the materials used are presented in Table 2.

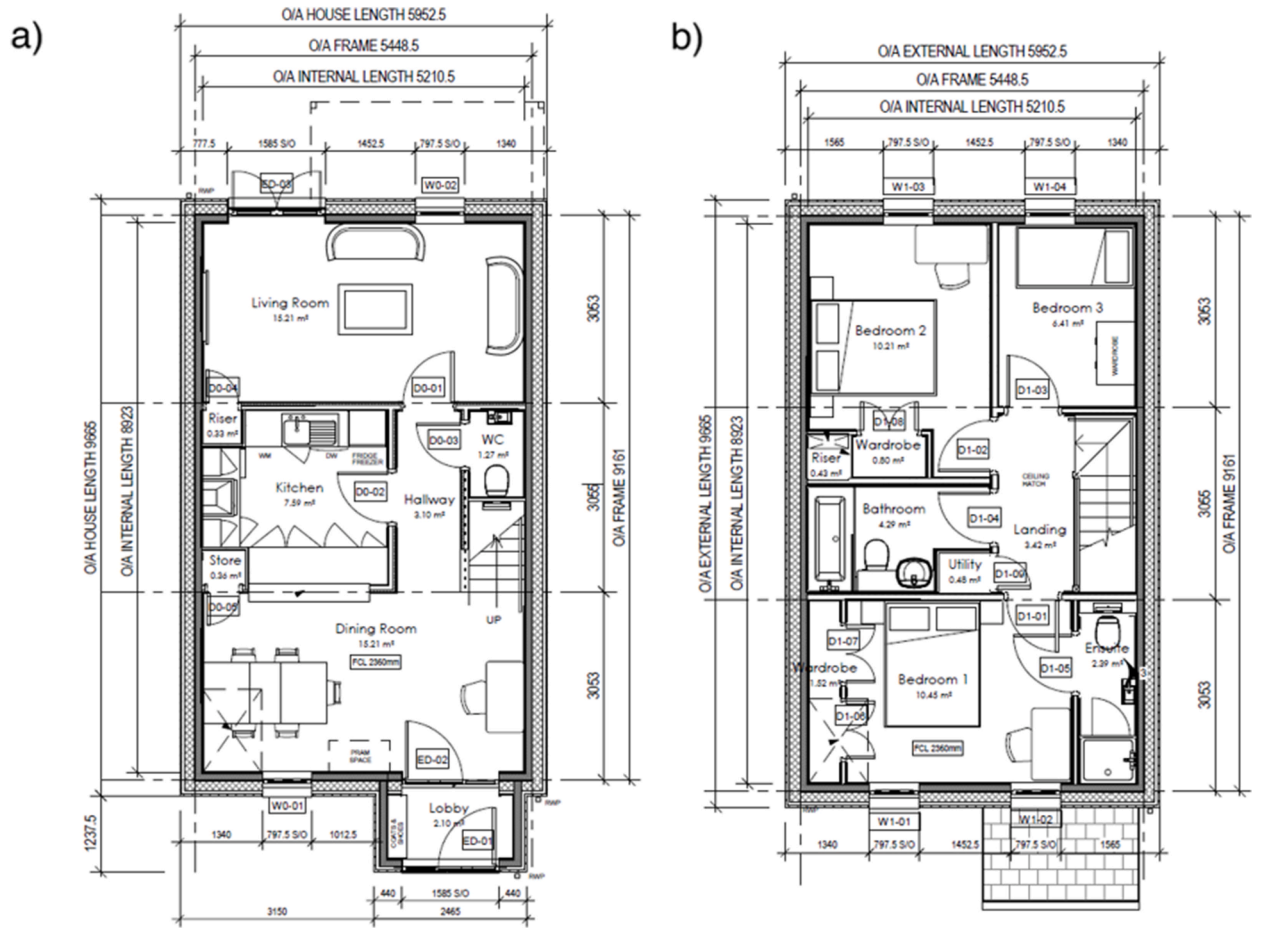

Fig. 7. Layout of typical superstructure: a) ground floor plan; b) first-floor plan.

Fig. 8. Piezometer and its system positioned outside the FAP modular system.

Table 1
Geometrical properties of the structural elements used for the proposed FAP system.

Element	Type	Width [mm]	Depth [mm]	Thickness [mm]	Class according to EC3
C45/100/45	beam	43	100	2	4
C45/100/45	column	43	100	2	4
C100/100/45	column	43	100	2	4
C100/200/100	beam	98	200	2	4
UB145	beam	48	145	2	4
UB175	beam	48	175	2	4
UB200	beam	48	200	2	4
UB255	beam	60	255	3	4
UB305	beam	60	305	3	4
Jack	column	–	101	19	1

Table 2
Mechanical properties of materials used for the proposed FAP system.

Elements	Material	Mass Density [kg/m^3]	Young's Modulus [MPa]	Poisson's Ratio [–]	Yield Strength [MPa]
Framing studs	Aluminium 6061	2700	68900	0.33	–
Outer cladding	Brick	1750	7000	0.20	–
Roof and floors	Plywood	23000	9400	0.40	–
Beams and columns	Z450 Galvanized steel	7850	200300	0.30	450
Jacks	S600 Steel	7850	210000	0.30	600

At rest (non-flooding occurrence), the FAP modular system rests on the ground, making the building appear like a typical house. Upon detecting rising water levels via a resilient piezometer installed on its base steel grid (Fig. 8), the system automatically activates hydraulic jacks to elevate the house up to 1500 mm at a slow speed of approximately 55 mm/min. Consequently, it takes 27 min for the Flood Adaptive Platform to reach its full height. According to the authors, there is limited information available on the speed of the onset of flooding, though some sources suggest flooding can rise at 60 mm/min. However, this is an extreme scenario not reflective of local climates like the UK's, where floodwater takes hours to rise over a meter. It is also worth noting that the motor's gearing ratios can be adjusted for faster lifting if needed, ensuring the current rate is globally more than sufficient. This system monitors, through continuous measurements, the water level during the occurrence of flooding, ensuring the safety of the property and preventing any part of the superstructure from coming into contact with floodwater. Building occupants can carry on with their usual activities without any disruption in their residences.

Once flooding stops, the FAP modular system returns to its starting position. During this phase, the sensors automatically check for obstructions, and if any are found, the FAP system will halt until they are removed. The elevation system can be activated either automatically or manually. In both cases, the user can decide the minimum vertical distance between the house and the water level, customising the elevation level according to their preferences and circumstances.

3. Loading scenarios adopted for the structural performance assessment

The efficiency and structural integrity of the newly developed structural system were assessed in a detailed manner. Vertical loadings, water loadings, wind action and seismic ground motions were utilised to assess the structural response of the proposed FAP modular system.

3.1. Gravity loads

The floor loading was calculated in accordance with Eurocode 1 [40] for residential buildings. A code-based value of 2.0 kNm^2 was utilised for each floor, while an additional loading of 2.0 kNm^2 was applied on the stairs. It is assumed that the roof of the building is not accessible except for maintenance, thus the loading value of 1.0 kNm^2 was used in the performed structural analyses.

3.2. Flood actions

As far as the flooding effects on structures are concerned, Eurocode 1 [40] provides a formula to calculate the horizontal force exerted by currents on vertical surfaces. However, this formula focuses on the total horizontal force and does not provide a detailed distribution of the pressure along the vertical element. Such detailed distribution is critical for accurately modelling the structural element in finite element analysis (FEA) applications. Therefore, the flooding actions were evaluated using the approach implemented in ASCE/SEI 7-05 [41], which separately evaluates the hydrostatic and hydrodynamic actions. The former action was evaluated with the following:

$$P_{stat} = g \cdot \gamma \cdot h \tag{1}$$

where g is the acceleration due to gravity (9.81 m/s^2), γ is the unit weight of water (1.0 kN/m^3), and h is the height at which the house stands measured from the ground or, alternatively, the height of the jacking system.

A maximum water flow velocity of 3 m/s was considered to calculate the hydrodynamic actions due to flood. Such value represents a water velocity threshold that indicates a moderate or extreme hazard to structures, depending on the water level [42]. As per the ASCE/SEI 7-05 [41], provisions, such value of water flow velocity allowed for the conversion of hydrodynamic action into constant hydrostatic action by increasing the flow depth by an amount equal to d_h, which was evaluated using:

$$d_h = \frac{a \cdot V^2}{2g} \tag{2}$$

where a is the drag coefficient equal to 1.2 for round piles, V is the average velocity of water in m/s, and g is the acceleration due to gravity. The resulting quantity was added to the headwater side of the jacks, which produced the pressure diagram shown in Fig. 9.

3.3. Wind actions

The wind pressures acting on the modular steel structural system were evaluated using Eurocode 1 [40]. Such housing system was assumed to be located in an area in the north of England with a fundamental wind velocity value of 25 m/s, corresponding to one of the highest in the UK as specified in the National Annex [43]. The wind pressures (w_e) acting on the external surfaces of the jack system were determined using the procedure outlined in Eurocode 1 [40], specifically using:

$$w_e = q_p\left(z_e\right) \cdot c_{pe} \tag{3}$$

where $q_p(z_e)$ is the peak velocity pressure, z_e is the reference altitude for the external pressure and c_{pe} is the pressure coefficient for the external pressure. The value of the wind pressure is directly related to the fundamental value of the basic wind speed. As the basic wind speed increases, the pressure also increases proportionally. The loads due to flooding and wind effects were combined using the ultimate limit state combination (ULS) specified in Eurocode 1 [40]. To fully investigate the structural behaviour of the FAP modular system, three height configurations were studied: 300 mm, 600 mm, and 900 mm, representing various flood risk scenarios defined by the Environmental Agency for surface water flood risk in the UK [6]. The computed loading values are summarised in Table 3.

The flood water velocity and wind action values correspond to upper-bound values for a conservative estimate of the structural safety assessment of the proposed FAP system. It should be noted, however, that it is unlikely that the computed maximum values are synchronous, however, it is believed that the performance assessment of the structural system under extreme loads may provide an adequate evaluation of the global structural robustness.

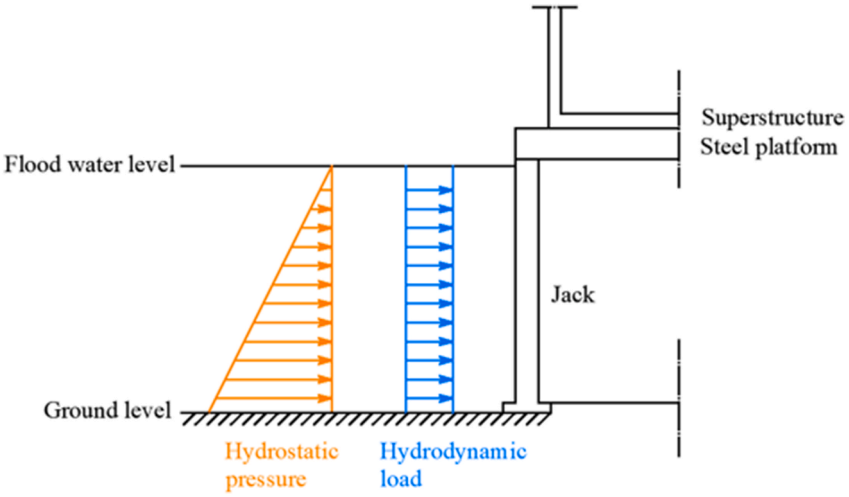

Fig. 9. Flood forces distribution acting on the jacking system.

Table 3
Ultimate State Limit horizontal loads for each configuration analysed.

ULS Load	300 mm configuration [kN/m^2]	600 mm configuration [kN/m^2]	900 mm configuration [kN/m^2]
Wind - side walls	0.58	0.59	0.59
Wind - short walls	0.36	0.37	0.37
Wind - roof	0.29	0.29	0.30
Hydrostatic	2.65	5.29	7.94
Hydrodynamic	7.50	10.14	12.79

3.4. Earthquake loads

The proposed innovative FAP modular system was also assessed when subjected to seismic ground motions, acting horizontally in both longitudinal and transverse directions (Fig. 5).

Strong motion records were selected using REXEL, a software that records the selection of real accelerograms based on the compatibility of displacement spectra [44]. REXEL utilises various databases, including the European Strong-motion Database (ESD). The selection of appropriate seismic ground motions was carried out with reference to the dynamic (modal) response of the modular steel structural system, e.g., fundamental frequencies of vibration. Table 4 provides details of the ground motions selected using REXEL, along with their corresponding peak ground acceleration (PGA) values for both horizontal directions. Fig. 10 shows the ground motion accelerograms and elastic spectra in the two directions of interest.

Table 4
PGA for earthquakes selected for the parametric analysis.

Earthquake	Date	Epicentral Distance [km]	Mw [–]	PGA in X direction [g]	PGA in Z direction [g]
Erzincan	December 27, 1939	13	6.6	3.81	5.03
Campano Lucano	November 23, 1980	16	6.9	1.53	1.72
South Iceland	June 17, 2000	7	6.5	6.14	5.02
Ano Liosia	September 07, 1999	18	6.0	1.09	0.84
Montenegro (1)	April 15, 1979	24	6.9	2.88	2.36
Montenegro (2)	April 15, 1979	16	6.9	3.68	3.56
Montenegro (aftershock)	May 24, 1979	20	6.2	0.56	0.54

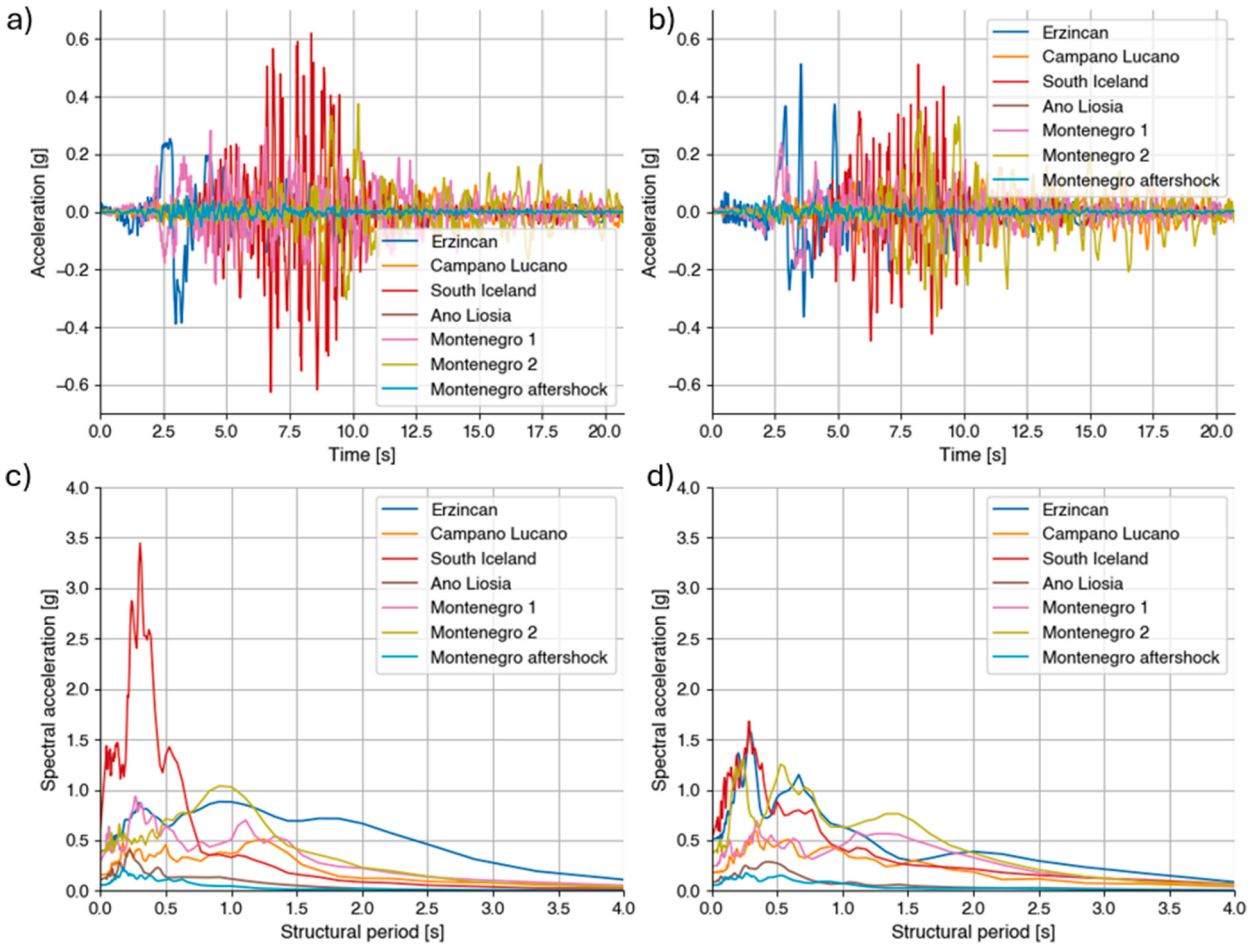

Fig. 10. Ground motions accelerograms in a) X and b) Z directions; elastic spectra in c) X and d) Z directions.

4. Numerical simulation for structural performance assessment

The modular steel building was modelled using Abaqus/CAE, a comprehensive software suite for FEA and computer-aided engineering. Three height configurations were studied: 300 mm, 600 mm, and 900 mm, which allowed for the thorough evaluation of the FAP system behaviour and response.

The initial step on Abaqus involved modelling over a hundred individual components of the FAP system as 3D deformable elements. Hence, the geometric characteristics of each component were determined, ensuring a balance between accuracy and computational efficiency. This involved representing elements with complex shapes or cross-sections in a simplified form, enabling reasonable analysis times while maintaining the accuracy of the results.

In the property module, the materials specified in Table 2 were defined and assigned to the parts previously defined. The elements composing the superstructure and the steel base grid were modelled with elastic behaviour, while the jacking system elements have a perfectly plastic elastic stress-strain curve, allowing them to enter the plastic field under significant stresses.

Once the geometric and mechanical characteristics of the FAP system were defined, the latter were assembled in the assembly module to create the complete system. The assemblies created within Abaqus/CAE were then meshed in the mesh module. For the jacks, vertical elements, and vertical threaded, tetrahedral elements (C3D10) were used with a density targeting an aspect ratio of 1. This choice aimed to achieve a higher accuracy of the results for these elements. The remaining elements of the jacking system, as well as those composing the superstructure and the steel base grid, were meshed using quadrilateral elements (C3D8R) with the highest aspect ratio equal to 12.

The analysis procedure and its steps were defined using the step module. The "Static, General" analysis was chosen to study the FAP system behaviour under gravity loads, flood loads, and wind action since the problem involved static loads and the time-dependent effects were negligible. This type of analysis leads to an accurate evaluation of structural behaviour under static loading conditions.

The loads were applied incrementally during the analysis; the maximum number of increments and small increment sizes were specified to ensure convergence and accurate results. Three separate "Static, General" steps were defined. In the first step, vertical loads were applied to the structure. In the second step, water loads acting on the jacking system were applied to simulate flood conditions. In the third step, wind action was applied. Depending on the analysis being performed, one or more steps could be activated or deactivated. By breaking down the analysis into different steps, it was possible to assess the individual effects of each load case on the structure, providing a clear understanding of their impact on the system's behaviour.

In the interaction module, the connections between the different elements of the modelled FAP modular system were defined as "ties". The ties represent bonded connections and were used to model the behaviour of both welded and bolted connections in the physical system. These ties allow for the transfer of loads and displacements between the connected surfaces or nodes, ensuring they act as a unified entity.

Boundary conditions were imposed on the base plates of the jacks using three-dimensional constraints. These constraints effectively prevented rotation and translation along the three reference axes, ensuring that the base plates remained fixed in their position. The dynamic behaviour of the system, namely natural vibration frequencies and mode shapes, was also investigated through a "Frequency, Linear Perturbation" analysis.

For the seismic analysis, ground motions were applied to the footings of each jack in the horizontal directions of the base metal grid. Multiple runs were considered to investigate the impact of individual actions as well as the combined effects of different load combinations. The implemented process may reliably simulate the FAP housing system under different scenarios, considering various floodwater heights and applied loads, as well as investigating the dynamic properties of the system to assess its response to seismic actions.

The implementation and calibration of the FAP modular system in Abaqus represented the second step of studying the behaviour of this system under multiple natural hazards (Fig. 11), which was achieved by comparing numerical results with those from HR Wallingford tests conducted in the previous phase. Following calibration, the numerical analyses shed light on structural response, ultimately yielding fragility curves for the three configurations studied for the FAP housing system.

5. Performance assessment evaluation

5.1. Safety factors for the Flood Adaptive Platform uplifting system at different heights above ground and different load combinations

The comprehensive numerical analyses were carried out by encompassing four load conditions to evaluate the behaviour of the FAP uplifting system under various scenarios. The first load condition, referred to as “G” (gravity loads), involved the application of gravitational loadings as specified in Eurocode 1 [40]. Such loads, which are always present, represent the constant forces exerted on the structure due to the weight of its components, irrespective of flood or wind conditions. An additional load condition, denoted as “G + H” (gravitational + hydrodynamic loads), incorporated both gravitational loads and the hydrostatic/hydrodynamic water loads associated with flooding. Such loads were applied to the surfaces of the jacks, considering different heights of the FAP system. The third load condition, named “G + W” (gravitational + wind loads), focused on the interaction between gravitational loads and wind forces. This scenario assumed no flooding, meaning the system was subjected solely to wind action as a natural hazard action. Lastly, the fourth load configuration, designated as “G + H + W”, accounted for all three types of loads: gravitational, hydrostatic/hydrodynamic water, and wind. This configuration represented a scenario where the FAP system experienced simultaneous flooding, high wind conditions and gravitational loads. Each of these load configurations was studied for three different heights of the jack system: 300 mm, 600 mm, and 900 mm from the ground, while the gravitational loads remain constant regardless of the height of the jacks,

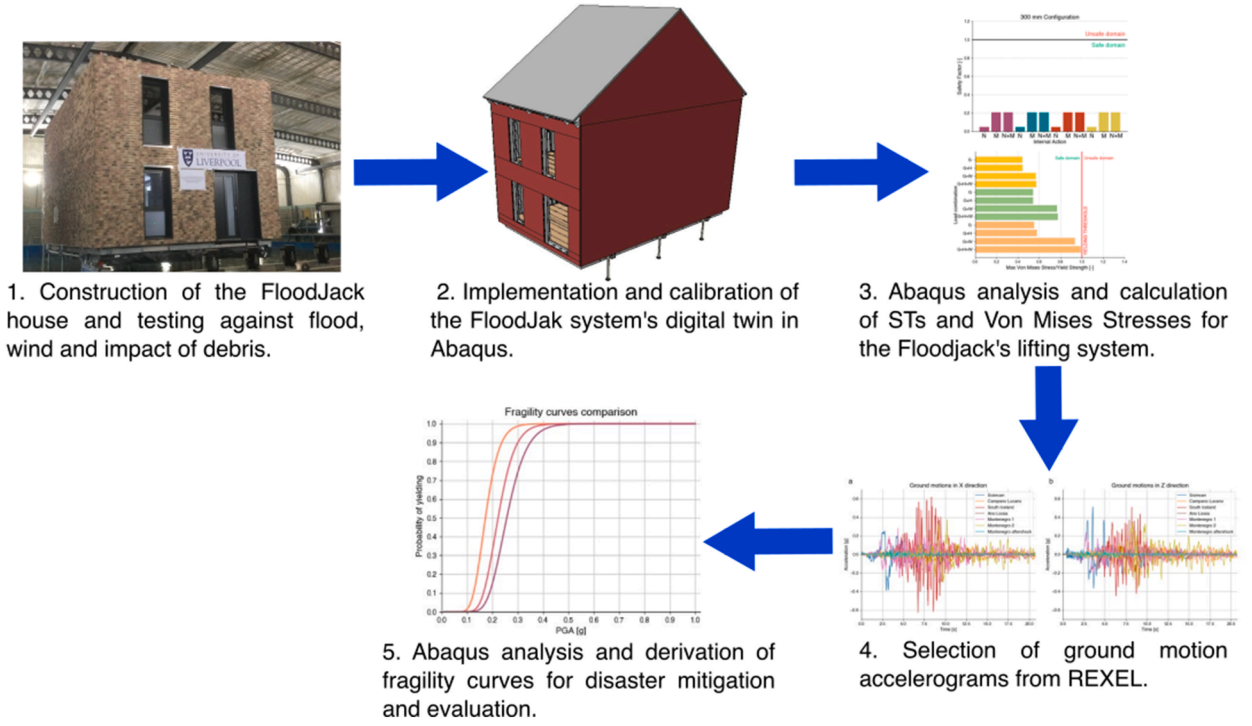

Fig. 11. Evaluation of the FAP system performance.

both the flood load and wind action are influenced by the height of the structure. As the height increases, these loads also increase. Besides the different loadings and the varying heights of the jacking system, all other parameters and characteristics of the model remained unchanged. This ensured that the loads and heights were the only variables influencing the behaviour of the system in these numerical analyses.

Fig. 12 shows the safety factors (SFs) for the different load conditions and two different heights of the FAP system, 300 mm and 900 mm. The SF is a dimensionless value obtained by comparing the maximum stress acting on the most heavily loaded jacks to its resistance calculated in accordance with Eurocode 3 [37]. It serves as a measure of the structural capacity and indicates how much margin of safety exists between the applied stresses and the material resistance. A SF equal or lower than 1,0 indicates that the structure is safe, as the resistance exceeds the applied stress. Conversely, a SF greater than 1,0 suggests that the applied stress approaches or exceeds the material capacity, indicating a potential failure risk of the analysed system.

Different SFs were evaluated for axial compression loads (N), bending moment (M), and the combination of axial load and bending moment (N + M). For the 300 mm height configuration, there is minimal variation in the SFs for the four load combinations. The

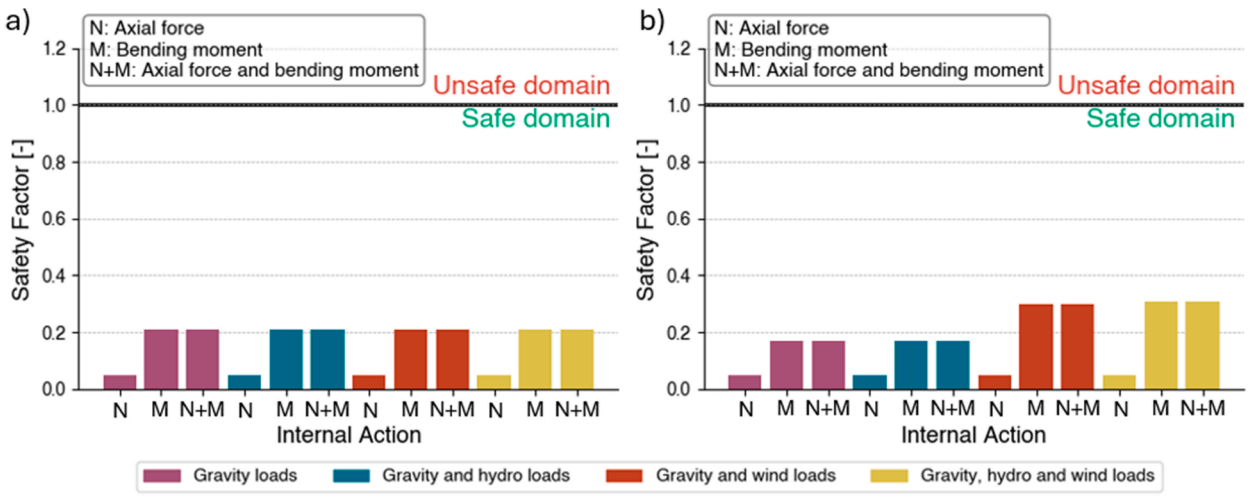

Fig. 12. Safety factor coefficient evaluated for a) 300 mm configuration and b) 900 mm configuration.

SFs for normal stress are less than 0.1, indicating that the compression capacity of the jacks is less than 10% utilised. The SFs for bending moment and the combination of bending moment and axial force remain relatively constant and slightly exceed 0.2. The values of the SFs for normal forces remain consistent across all load combinations, even as the FAP housing system moves from 600 mm to 900 mm. However, as the height increases, SFs for bending moment and the combination of bending moment and axial load show an increase for "G + W" and "G + H + W" load conditions compared to "G" and "G + W" load conditions. This trend is more pronounced at a height of 900 mm. This indicates the sensitivity of the structure's safety to wind loads, particularly as the height increases. As the height of the FAP system increases, the influence of wind loads becomes more significant, resulting in higher SFs and thus indicating a reduced safety margin. This suggests that wind action plays a more critical role in the structure's safety. However, it is important to note that even in these cases, the SFs do not exceed 0.4, indicating that the structure remains far from failure and within safe limits.

5.2. Local stress (Von Mises) analysis for the Flood Adaptive Platform system at different heights above ground and different load combinations

Fig. 13 shows the ratio between the maximum Von Mises stress experienced by the most heavily loaded jack and the yield strength of the jack, which is 600 MPa, for each load condition and the three different heights of the FAP system. The Von Mises stress represents the combined effect of normal and shear stresses on the material. If the dimensionless ratio is less than 1,0, then the system is in the elastic range (no plasticisation), meaning it has not exceeded its yield strength. However, if the ratio equals or exceeds 1,0, it signifies plasticisation, indicating permanent plastic deformation (Fig. 14). In the latter case, the jack system would no longer provide effective protection against flooding, as the permanent deformation would prevent it from returning to its initial position.

The lowest value of the ratio is observed when only gravitational and combined gravitational and flood loads are applied to the system. These ratios tend to increase as the structure is raised, moving from slightly more than 0.4 to just under 0.6 for the 900 mm configuration. A significant increase in the ratio is attributed to wind loads. As the height of the FAP system increases, the impact of wind actions becomes more significant, reaching the highest stress ratios for the tallest configuration, highlighting once again the structure's sensitivity to wind action. Although the influence of water action is less pronounced, it also plays a role in the definition of the ratio. The combined application of gravitational, wind, and water loads results in the most reduced safety margin, with stress ratios nearing unity but not reaching plasticisation.

5.3. Fragility analysis of Flood Adaptive Platform system

Fragility functions express the likelihood of a structure reaching or surpassing a certain level of damage as a function of the intensity of the seismic activity. Through graphical representation, they serve as a direct means to make well-informed decisions and assess the susceptibility of a structural system to earthquakes, helping engineers, stakeholders and policymakers. Depending on the way such functions are obtained, there are three main types of fragility functions: empirical, analytical and hybrid [45,46]. The former are obtained through observational data; hence, they are considered realistic. However, such type of fragility curves can be limited in

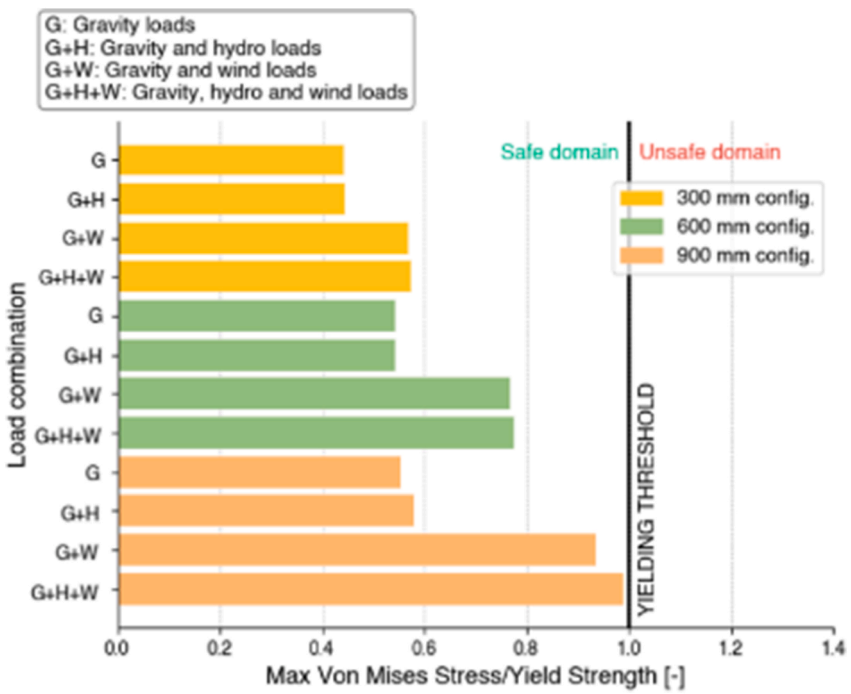

Fig. 13. Ratio of maximum Von Mises stress to yield stress of steel. The ratios were calculated for different load conditions and different heights of the FAP system.

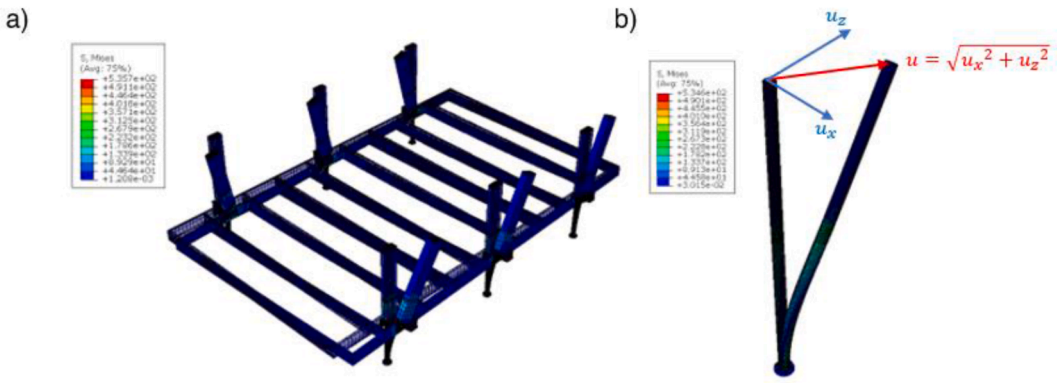

Fig. 14. a) deformed jacking system and steel base grid; b) deformed jack.

availability, especially at low seismic intensity levels. Analytical fragility functions are instead constructed using mathematical models and can encompass various structural configurations and environmental factors. They principally aim to minimise bias but may have limitations related to software modelling. Hybrid fragility functions are a combination of empirical and analytical curves. They are used to compensate for modelling difficulties, combine different data sources, and reduce uncertainty. Thus, they are particularly useful when observational data for different structural configurations are lacking. Fragility functions are characterised by their typical "S"-shaped form, signifying that structures generally withstand lower levels of ground shaking with greater resistance but become more susceptible as shaking intensity increases. This nonlinear shape also emphasises the presence of uncertainty regarding whether a limit state is breached. Consequently, fragility functions can indicate both lower and higher probabilities. Alternatively, a deterministic scenario with no uncertainty can arise, where the probability of reaching a limit state is either one or zero, resulting in a fragility function resembling a step function. In this study, fragility functions were developed using the analytical methodology proposed by Baker [47] to compare the vulnerability of the FAP system at three different configurations: 300 mm, 600 mm and 900 mm.

According to the latter methodology, analytical fragility functions adapted for the present case are represented by the following lognormal cumulative distribution function:

$$P\left(Pl \mid PGA = x\right) = \Phi\left(\frac{\ln\left(\frac{x}{\mu}\right)}{\beta}\right) \tag{4}$$

where $P(Pl \mid IM = x)$ is the probability of reaching the plasticisation of the jacks when a ground motion with peak ground acceleration (PGA) $PGA = x$ is occurring, Φ is the standard normal cumulative distribution, μ is the PGA level with 50% probability of collapse and β is the dispersion of the PGA. Fragility functions are thus defined once the μ and β parameters are obtained. In this case, such parameters were estimated through the maximum likelihood method and performing several analyses in Abaqus at a discrete set of PGA levels, with different ground motions used at each PGA level. The maximum likelihood method finds parameters such that the resulting probability distribution is the one with the highest likelihood of producing the observed data, in this case, the plasticisation of the jacks. For each PGA level x_i, the probability of observing z_i collapses out of n_i ground motions is given by the following binomial distribution:

$$P\left(z_i \; collapses \; in \; n_i \; ground \; motions\right) = \binom{n_i}{z_i} \cdot {p_i}^{z_i} \cdot \left(1 - p_i\right)^{n_i - z_i} \tag{5}$$

where p_i is the probability that a ground motion characterised by a PGA x_i will cause the plasticisation of the jacks, also defined as $P(Pl \mid IM = x)$ in Eq. (4). Through the maximum likelihood approach, p_i is defined as the probability function that maximises the probability of having observed the collapse data that was obtained from the Abaqus analyses. Given that the plasticisation of the jacks has been observed at various PGA levels, we can reformulate Eq. (5). This reformulation incorporates the multiple m levels of PGA where jack collapse incidents have occurred, deriving the corresponding likelihood.

$$Likelihood = \prod_{i=1}^{m} \binom{n_i}{z_i} \cdot {p_i}^{z_i} \cdot \left(1 - p_i\right)^{n_i - z_i} \tag{6}$$

where Π represents the product over all m levels. Replacing Eq. (4) for p_i we then have:

$$Likelihood = \prod_{i=1}^{m} \binom{n_i}{z_i} \cdot \Phi\left(\frac{\ln\left(\frac{x_i}{\mu}\right)}{\beta}\right)^{z_i} \cdot \left(1 - \Phi\left(\frac{\ln\left(\frac{x_i}{\mu}\right)}{\beta}\right)\right)^{n_i - z_i} \tag{7}$$

Therefore, estimates of the fragility curves parameters μ and β are obtained by maximizing the latter likelihood function.

The fragility curves were generated by subjecting the structure to seismic accelerations in the horizontal directions X and Z, as well as gravitational loads. The chosen ground motions were scaled to have a maximum PGA value relative to the two horizontal directions, multiplied by a factor of 0.05 g. Starting from this scaled acceleration, the structural response of the system, particularly the jacking system, was analysed to ensure that no element reached plasticisation.

Each of the seven seismic inputs was incrementally increased, and analyses were conducted until plasticisation occurred in one of the jacks. From the fragility curves presented in Fig. 15, it can be observed that the structural response of the system to seismic action is generally mediocre. When the superstructure is raised to a height of 300 mm, its fragility curve begins to show a non-zero probability of damage at a PGA of 0.15 g. This means that at a seismic intensity of 0.15 g, there is a chance greater than zero that the structure will suffer some form of damage. The curve also demonstrates a gradual rise in the likelihood of damage as the PGA increases. When the PGA reaches 0.45 g, the probability of damage reaches unity, indicating a 100% chance that the structure will be damaged at this level of seismic activity. The values at which there is a non-zero probability of damage and a certain probability of damage become smaller as the height of the FAP house increases. At 900 mm, there is a non-zero probability of damage at a PGA of 0.1 g and a certain probability of damage at a PGA of 0.3 g. In Fig. 15d, it is clearly shown how the fragility curves change, and the probability of failure increases as the structure rises. Also, the values of the parameters μ and β were reported. A lower β implies a steeper curve with a

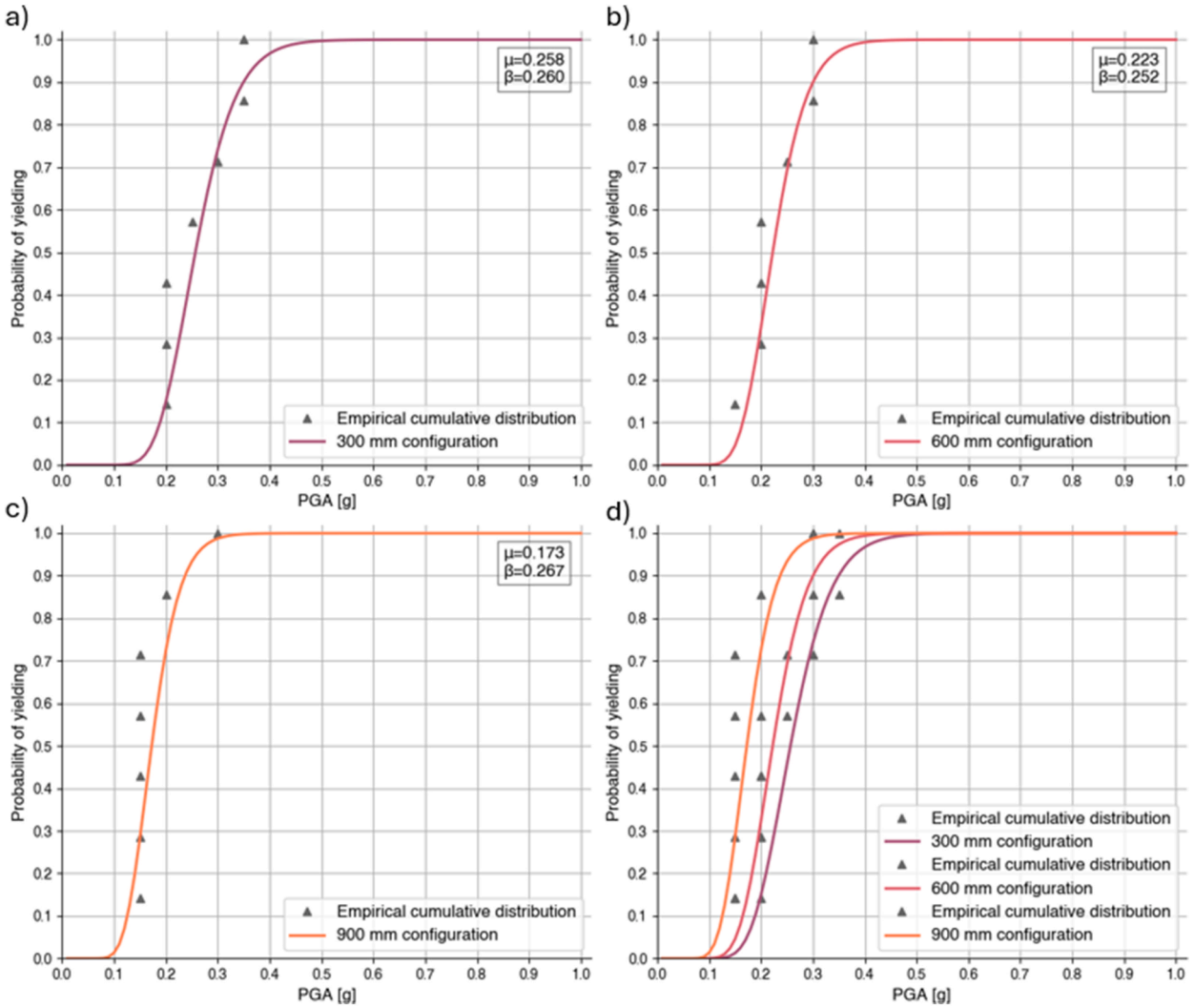

Fig. 15. Fragility curves for a) 300 mm configuration; b) 600 mm configuration; c) 900 mm configuration and d) fragility curves comparison.

steeper increase in vulnerability, while a higher β implies a shallower curve with a slower increase in vulnerability as the intensity of shaking increases. For the reasons mentioned above, the value of μ tends to decrease as the height of the FAP system increases, while the β parameter remains about the same.

6. Safe use of the Flood Adaptive Platform system for regional applications

The outcomes of the comprehensive numerical analyses illustrated in the previous paragraphs proved that the FAP system exhibited safe behaviour for all configurations in the different scenarios. Even when subjected to gravitational loads along with the additional forces from flood and wind actions, the system met the strength requirements outlined in Eurocode 3 [37], and no plasticisation of the jacking system was observed. The elastic response is crucial for the system operation, allowing it to be raised and lowered multiple times without any issues. Flood and wind actions considered in the analyses were not of minor magnitude, but rather represented near-maximum values that could occur during such weather events.

The behaviour of the FAP house under minor wind speeds was further investigated. Eurocode 3 [37] divides the territory of the United Kingdom into bands characterised by a specific average wind speed. The higher the average wind speed, the greater the pressure on the outer surfaces of the building. In this case, average reference wind speeds of 22, 23 and 25 m/s were considered, as shown in Fig. 16. Therefore, from each of these average wind speeds, the values of the pressure acting on the faces of the FAP system were obtained, and the analyses were conducted in Abaqus, determining the ratio between the maximum stress according to Von Mises and the yield strength. For each configuration of the FAP modular system, these ratios are shown in Table 5. In this calculation, the safety

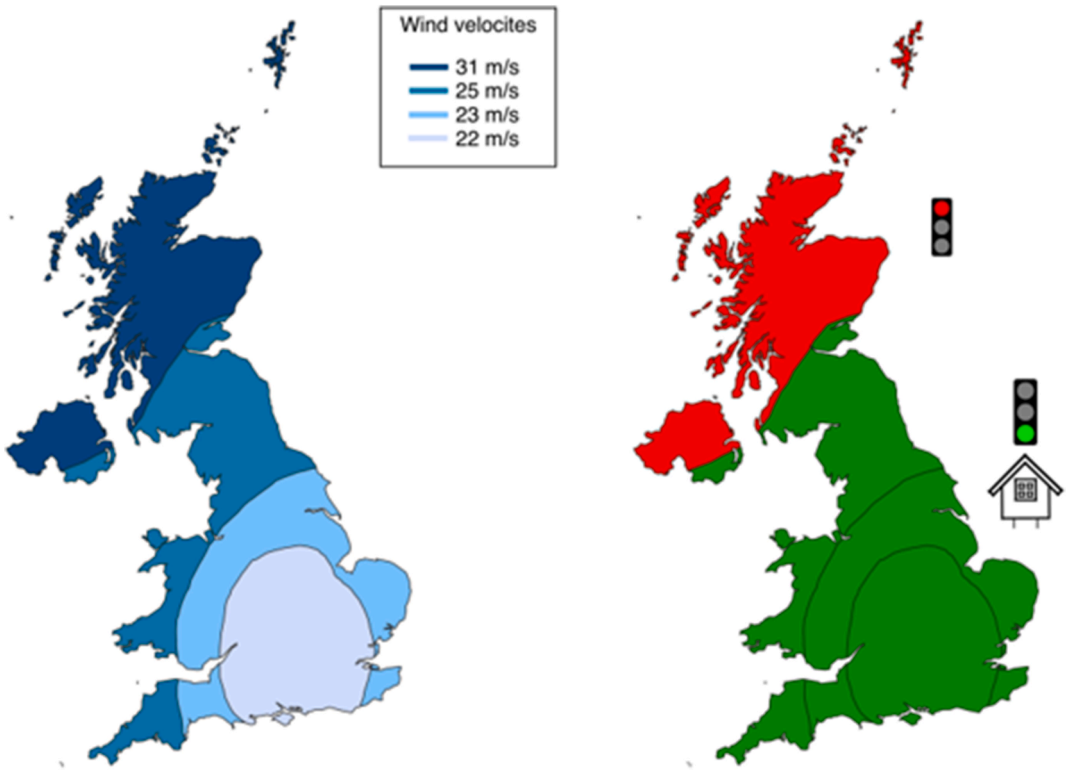

Fig. 16. Feasibility of the use the FAP modular system in the UK for the joint wind-flood hazard: average wind speed in the UK according to Eurocode 3 (left) and areas where the innovative FAP system can be safety employed to natural hazards due floods and wind (right).

Table 5
Ratio of maximum Von Mises stress to yield stress of steel. The ratios were calculated for different load conditions, different average wind velocity and different heights of the FAP system.

Load combination	300 mm configuration			900 mm configuration		
	22 m/s	23 m/s	25 m/s	22 m/s	23 m/s	25 m/s
G	0.44	0.44	0.44	0.56	0.56	0.56
G + H	0.45	0.45	0.45	0.58	0.58	0.58
G + W	0.55	0.55	0.57	0.80	0.85	0.94
G + H + W	0.55	0.55	0.58	0.83	0.89	0.99

factors in relation to the stress acting on the jacks were also not calculated, because the verification, as can be seen from Fig. 13, is verified for the highest velocity value.

Regarding the seismic response of the system, it exhibited discernible behaviour. The height at which the system is elevated influences its dynamic response, with the structure being more susceptible to earthquakes when raised higher off the ground.

Based on the results of the detailed numerical analyses carried out herein, it can be concluded that the FAP system is a viable solution for areas prone to multiple natural hazards such as wind, flood, and earthquakes. Therefore, it has potential applications in regions where one or more of these phenomena occur altogether, such as Indonesia, China, Central America and Central Europe.

7. Conclusive remarks and future actions

This paper illustrates the causes of natural floods, emphasising social consequences and economic cascading effects. Floods are increasingly costly due to climate change, prompting the adoption of various mitigation techniques. At the property level, such strategies comprise flood-avoidance, resistance, and resilience, thus minimising the impact of floodwater on structures. A viable, sustainable, and resilient flood mitigation method is the innovative FAP system, which has been presented in previous paragraphs. This structural steel modular system employs mechanical jacks to elevate the superstructure, preventing contact with floodwater and ensuring functionality during and after flood events. This game-changing technology can also be adopted to protect critical components for essential facilities, such as hospital buildings, schools, and nuclear reactors.

The FAP system has effectively addressed several potential challenges to its real-world implementation. Community acceptance has been initially positive, particularly in high-risk flooding areas, and is expected to grow as the technology is deployed. The National Planning Policy Framework in England presents regulatory challenges for new residential builds in high-risk areas, but there are fewer barriers in the mobile home and holiday lodge sectors. Additionally, the system meets all UK regulatory requirements, including compliance with building regulations and National House Building Council warranties, which assure high construction standards and provide warranties for new homes. Insurance considerations are addressed through full product warranties, service agreements, and product and public liability insurance, which could potentially lower insurance premiums over time. The cost of the system, while significant (approximately £ 31,500 for a residential house), is competitive compared to the average cost of flood damage in the UK (around £ 60,000), making it a viable economic option. Thus, the challenges of community acceptance, regulatory approvals, and cost have been well-tackled, ensuring the feasibility and acceptance of the FAP system in various sectors.

Physical tests, including hydraulic water-pressure actions, wind loading, and impact tests, were conducted at the state-of-the-art testing facility HR Wallingford in Oxfordshire, UK, to assess the safety of the innovative modular steel building system. It was found that the structural performance of the tested full-scale specimen was compliant with modern guidelines for flood-resilient building structures. The system is easy to use due to its low-energy demand during operations and low maintenance requirements for the jack system.

A digital twin computational model, calibrated on the refined outcomes of comprehensive experimental tests on the full-scale specimen, was implemented and utilised to optimise the FAP modular design to achieve a sustainable, cost-effective, yet efficient resilient structural system. Numerical analyses revealed the ability of the novel innovative modular steel system to withstand combined natural hazards, including floods, strong winds, and earthquakes, making it a valuable tool in flood-prone areas facing multiple threats. Future development will involve installing low-cost, energy-efficient, and self-harvested sensors within low-carbon bio-based panels of the claddings of the modular steel building, allowing remote real-time control of the jacking system, even when the users or occupants are off-site.

CRediT authorship contribution statement

Luigi Di Sarno: Writing – review & editing, Writing – original draft, Validation, Supervision, Resources, Project administration, Methodology, Investigation, Funding acquisition, Formal analysis, Data curation, Conceptualization. **Roberto Forgione:** Writing – original draft, Investigation, Formal analysis.

Declaration of competing interest

I can declare on behalf of my coauthor that we have no conflicting interests regarding submission of this manuscript to International Journal of Disaster Risk Reduction.

Acknowledgments

The research was partially funded through FLOod-RESilient modular system for affordable and sustainable houses (FLORES) project, as part of the European Regional Development Fund, Eco-I North West at University of Liverpool, UK.

Data availability

Data will be made available on request.

References

[1] Université catholique de Louvain (UCLouvain), Centre for research on the epidemiology of disasters (CRED), n.d.). Data accessibility. EM-DAT: The Emergency Events Database. (2024) Retrieved 14 June 2024, from. https://public.emdat.be/data.
[2] Centre for Research on the Epidemiology of Disasters (CRED), 2022 disasters in numbers. Brussels: centre for research on the epidemiology of disasters, Retrieved 14 June 2024, from. https://cred.be/sites/default/files/2022_EMDAT_report.pdf.
[3] S. Doocy, A. Daniels, S. Murray, T.D. Kirsch, The human impact of floods: a historical review of events 1980-2009 and systematic literature review, PLoS currents 5 (2013), https://doi.org/10.1371/currents.dis.f4deb457904936b07c09daa98ee8171a.
[4] Munich Re, Factsheet natural catastrophes in 2021, Retrieved 14 June 2024, from. https://www.munichre.com/content/dam/munichre/mrwebsiteslaunches/natcat-2022/2021_Figures-of-the-year.pdf/jcr_content/renditions/original./2021Figures-of-the-year.pdf.
[5] Munich Re, Natural disasters in 2022. Retrieved 14 June 2024, from, https://www.munichre.com/content/dam/munichre/mrwebsitespressreleases/natcat_stats_2022_factsheet.pdf/_jcr_content/renditions/original./natcat_stats_2022_factsheet.pdf.
[6] Environment Agency, Flooding in England: A National Assessment of Flood Risk, Environment Agency, 2009, pp. 1–36.
[7] W. Zhang, G. Villarini, G.A. Vecchi, J.A. Smith, Urbanization exacerbated the rainfall and flooding caused by Hurricane Harvey in Houston, Nature 563 (7731) (2018) 384–388, https://doi.org/10.1038/s41586-018-0676-z.
[8] S.B. Ajjur, S.G. Al-Ghamdi, Exploring urban growth–climate change–flood risk nexus in fast-growing cities, Sci. Rep. 12 (1) (2022), https://doi.org/10.1038/s41598-022-06022-4.
[9] A. Bronstert, Floods and climate change: interactions and impacts, Risk Anal. 23 (3) (2003) 545–557, https://doi.org/10.1111/1539-6924.00335.
[10] M.M. Mirza, Climate change, flooding in South Asia and implications, Reg. Environ. Change 11 (1) (2010) 95–107, https://doi.org/10.1111/1539-6924.00336.
[11] N.L. Poff, Ecological response to and management of increased flooding caused by climate change, Philos. Trans. R. Soc. London, Ser. A: Math. Phys. Eng. Sci. 360 (1796) (2002) 1497–1510, https://doi.org/10.1098/rsta.2002.1012.
[12] Y. Hirabayashi, et al., Global flood risk under climate change, Nat. Clim. Change 3 (9) (2013) 816–821, https://doi.org/10.1038/nclimate1911.
[13] E. Bichard, A. Kazmierczak, Are homeowners willing to adapt to and mitigate the effects of climate change? Climatic Change 112 (3–4) (2012) 633–654, https://doi.org/10.1007/s10584-011-0257-8.
[14] K. Calvin, et al., IPCC, 2023: Climate Change 2023: Synthesis Report. Contribution of Working Groups I, II and III to the Sixth Assessment Report of the Intergovernmental Panel on Climate Change, IPCC, Geneva, Switzerland, 2023.
[15] A. Abbas, T.S. Amjath-Babu, H. Kächele, M. Usman, K. Müller, An overview of flood mitigation strategy and research support in South Asia: implications for sustainable flood risk management, Int. J. Sustain. Dev. World Ecol. 23 (2) (2015) 98–111, https://doi.org/10.1080/13504509.2015.1111954.
[16] C.A. Bana e Costa, P. Antão da Silva, F. Nunes Correia, Multicriteria evaluation of flood control measures: the case of ribeira do livramento, Water Resour. Manag. 18 (3) (2004) 263–283, https://doi.org/10.1023/B:WARM.0000043163.19531.6a.
[17] L. Cea, P. Costabile, Flood risk in urban areas: modelling, management and adaptation to climate change. A review, Hydrology 9 (1) (2022) 50, https://doi.org/10.3390/hydrology9030050.
[18] Z.W. Kundzewicz, D.L. Hegger, P. Matczak, P.P. Driessen, Flood-risk reduction: structural measures and diverse strategies, Proc. Natl. Acad. Sci. USA 115 (49) (2018) 12321–12325, https://doi.org/10.1073/pnas.1818227115.
[19] V. Meyer, S. Priest, C. Kuhlicke, Economic evaluation of structural and non-structural flood risk management measures: examples from the Mulde River, Nat. Hazards 62 (2) (2011) 301–324, https://doi.org/10.1007/s11069-011-9997-z.
[20] B.M. Rehan, J.W. Hall, E.C. Penning-Rowsell, V.Z.H. Tan, A comparison of the cost effectiveness of property-level adaptation and community-scale flood defences in reducing flood risk, Journal of Flood Risk Management 17 (1) (2024) e12956, https://doi.org/10.1111/jfr3.12956.
[21] M.S.G. Adnan, A. Haque, J.W. Hall, Have coastal embankments reduced flooding in Bangladesh? Sci. Total Environ. 682 (2019) 405–416, https://doi.org/10.1016/j.scitotenv.2019.05.048.
[22] J.R. Zaman, C.E. Haque, D. Walker, Local-level flood hazard management in Canada: an assessment of institutional structure and community engagement in the Red River Valley of Manitoba, Geographies 2 (4) (2022) 743–768, https://doi.org/10.3390/geographies2040046.
[23] J.A. Klein, C.M. Tucker, C.E. Steger, A. Nolin, R. Reid, K.A. Hopping, E.T. Yeh, M.S. Pradhan, A. Taber, D. Molden, R. Ghate, D. Choudhury, I. Alcántara-Ayala, S. Lavorel, B. Müller, A. Grêt-Regamey, R.B. Boone, P. Bourgeron, E. Castellanos, K. Yager, An integrated community and ecosystem-based approach to disaster risk reduction in mountain systems, Environ. Sci. Pol. 94 (2019) 143–152, https://doi.org/10.1016/j.envsci.2018.12.034.
[24] R. Mechler, L.M. Bouwer, Understanding trends and projections of disaster losses and climate change: is vulnerability the missing link? Climatic Change 133 (1) (2015) 23–35, https://doi.org/10.1007/s10584-014-1141-0.
[25] O.M. Nofal, J.W. van de Lindt, H. Cutler, M. Shields, K. Crofton, Modeling the impact of building-level flood mitigation measures made possible by early flood warnings on community-level flood loss reduction, Buildings 11 (10) (2021) 475, https://doi.org/10.3390/buildings11100475.
[26] M.S. Attems, T. Thaler, E. Genovese, S. Fuchs, Implementation of property-level flood risk adaptation (PLFRA) measures: choices and decisions, Wiley Interdisciplinary Reviews: Water 7 (1) (2020) e1404, https://doi.org/10.1002/wat2.1404.
[27] CIRIA, Improving the Flood Performance of New Buildings: Flood Resilient Construction, Department for Communities and Local Government, London, England, 2007.
[28] C. Zevenbergen, A. Cashman, N. Evelpidou, E. Pasche, S. Garvin, R. Ashley, Urban Flood Management, Taylor & Francis Group, London, England, 2011.
[29] T. Egli, Wegleitung Objektschutz gegen gravitative Naturgefahren, Vereinigung Kantonaler Feuerversicherungen, Bern, Switzerland, 2005.
[30] FEMA, Homeowner's Guide to Retrofitting: Six Ways to Protect Your Home from Flooding, Federal Emergency Management Agency, Washington, DC, 2014.
[31] J.C.J.H. Aerts, W.J.W. Botzen, H. De Moel, M. Bowman, Cost estimates for flood resilience and protection strategies in New York City, Ann. N. Y. Acad. Sci. 1294 (1) (2013) 1–104, https://doi.org/10.1111/nyas.12200.
[32] H. Kreibich, P. Bubeck, M. Van Vliet, H. De Moel, A review of damage-reducing measures to manage fluvial flood risks in a changing climate, Mitig. Adapt. Strategies Glob. Change 20 (6) (2015) 967–989, https://doi.org/10.1007/s11027-014-9629-5.
[33] P. Bowker, Flood Resistance and Resilience Solutions: an R&D Scoping Study, Department for Environment, London, England, 2007 Food & Rural Affairs.
[34] J.K. Poussin, P. Bubeck, J.C.J.H. Aerts, P.J. Ward, Potential of semi-structural and non-structural adaptation strategies to reduce future flood risk: case study for the Meuse, Nat. Hazards Earth Syst. Sci. 12 (2012) 3455–3471, https://doi.org/10.5194/nhess-12-3455-2012.
[35] R. Lasage, T.I.E. Veldkamp, H. de Moel, T.C. Van, H.L. Phi, P. Vellinga, J.C.J.H. Aerts, Assessment of the effectiveness of flood adaptation strategies for HCMC, Nat. Hazards Earth Syst. Sci. 14 (2014) 1441–1457, https://doi.org/10.5194/nhess-14-1441-2014.
[36] E. English, C. Friedland, F. Orooji, N. Mahtani, A New Approach to Combined Flood and Wind Mitigation for Hurricane Damage Prevention, Paper presented at the 14th International Conference on Wind Engineering, Porto Alegre, Brazil, 2015.
[37] British Standards Institution, BS EN 1993-1-1:2005 +A1:2014. Eurocode 3: Design of Steel Structures – Part 1-1: General Rules and Rules for Buildings, BSI, 2015.
[38] A.W. Lacey, W. Chen, H. Hao, K. Bi, Structural response of modular buildings – an overview, J. Build. Eng. 16 (2018) 45–56, https://doi.org/10.1016/j.jobe.2017.12.008.
[39] A. Fathieh, O. Mercan, Seismic evaluation of modular steel buildings, Eng. Struct. 122 (2016) 83–92, https://doi.org/10.1016/j.engstruct.2016.04.054.
[40] British Standards Institution, BS EN 1991-1-1:2002. Eurocode 1: Actions on Structures – Part 1-1: General Actions – Densities, Self-Weight, Imposed Loads for Buildings, BSI, 2002.
[41] American Society of Civil Engineers/Structural Engineering Institute, ASCE/SEI 7-05. Minimum design loads for buildings and other structures, ASCE/SEI (2006).
[42] G.P. Smith, E.K. Davey, R. Cox, Flood Hazard. WRL Technical Report 2014/07, Water Research Laboratory – University of New South Wales, 2014.
[43] British Standards Institution, UK National Annex to Eurocode 1: Actions on Structures. NA to BS EN 1991-1-4:2005, BSI, 2008.
[44] C. Smerzini, C. Galasso, I. Iervolino, R. Paolucci, Ground motion record selection based on broadband spectral compatibility, Earthq. Spectra 30 (4) (2014) 1427–1448, https://doi.org/10.1193/052312EQS197M.

[45] K. Porter, R. Kennedy, R. Bachman, Creating fragility functions for performance-based earthquake engineering, Earthq. Spectra 23 (2) (2007) 471–489, https://doi.org/10.1193/1.2720892.
[46] L. Di Sarno, A.S. Elnashai, Seismic fragility relationships for structures, in: Springer Tracts in Civil Engineering, 2021, pp. 189–222, https://doi.org/10.1007/978-3-030-68813-4_9.
[47] J.W. Baker, Efficient analytical fragility function fitting using dynamic structural analysis, Earthq. Spectra 31 (1) (2015) 579–599, https://doi.org/10.1193/021113EQS025M.